行政院國家科學委員會專題研究計畫 成果報告

修正碳分子篩選薄膜之微孔結構及其於氣體分離特性之應用
研究成果報告(精簡版)

計 畫 類 別 ：個別型
計 畫 編 號 ：NSC 96-2221-E-040-001-
執 行 期 間 ：96 年 08 月 01 日至 97 年 10 月 31 日
執 行 單 位 ：中山醫學大學職業安全衛生學系暨碩士班

計 畫 主 持 人：曾惠馨

計畫參與人員：博士班研究生-兼任助理人員：庫馬

報 告 附 件 ：出席國際會議研究心得報告及發表論文

公 開 資 訊 ：本計畫涉及專利或其他智慧財產權，2 年後可公開查詢

中 華 民 國 98 年 01 月 31 日

Novel SBA-15/carbon nanocomposite membrane with high permeance for gas separation

Hui-Hsin Tseng [a,*], Pei-Ting Shiu [a], Yi-Shan Lin [a], Itta Arun Kumar [b]

[a] *Department of Occupational Safety and Health, Chung Shan Medical University, Taichung, Taiwan*

[b] *Department of Environmental Engineering, National Chung Hsing University, Taichung, Taiwan*

*Corresponding author: Tel.: +886-4-24730022; Fax: +886-4-23248194.

E-mail address: hhtseng@csmu.edu.tw (H.-H. Tseng)

Abstract

Novel zeolite SBA-15/carbon nanocomposite membrane using polyetherimide (PEI) as precursor were successfully prepared by spin coating method for gas transport. Thermo gravimetric analysis (TGA) and field emission scanning electron microscopy (FESEM) were employed to characterize the nanocomposite membrane structure properties. In single gas permeation experiments, the zeolite SBA-15/carbon nanocomposite membrane exhibited excellent carbon dioxide permeance of 49.3 Barrer with ideal separation factor of CO_2/N_2 of 27.4 at room temperature and 2 atm. Based on TGA and FESEM investigations, the membranes appear more microporous structure while incorporated with SBA-15 zeolite. These results supported that zeolite improve gas diffusivity by increasing the micropore volume.

Keywords: carbon membrane; gas separation; polyimide; zeolite; carbonization

1. Introduction

Membrane separation processes has become one of the emerging technologies, which have undergone a rapid growth during the last few decades [1-3]. Recently inorganic membranes such as micro and mesoporous silica membranes [4], zeolite membranes [5], and carbon molecular sieve (CMS) membranes [6-7] were quickly developed and they offer outstanding potential such as greater mechanical strength, chemical inertness, high temperature stability and time-independent performance for gas separation applications [8].

Among these inorganic membranes, CMS membrane has been recognized as an attractive gas separation material due to have shown permeation and separation properties significantly exceeding those of their polymeric precursor membranes [9-12]. In CMS membrane with pores approaching the molecular diameters of the gases to be separated (<6Å), the main mechanism is molecular sieving. The separation takes place on the basis of size exclusion and is therefore not dependent on pore wall-gas molecule interactions nor on the feed pressure [9].

CMS membrane are usually fabricated by carbonization of suitable polymeric precursors such as polyimide [13-16], polyacronitrile [17], phenolic resin [18-19] polyfurfuryl alcohol (PFA) [20-22], Polyetherimide [23], Poly vinylidene chloride

co-vinyl chloride (PVP) [24]. In general, polymeric membrane preparation conditions, pre-treatment of the precursor, pyrolysis conditions, and post-treatment of pyrolysed membranes are all play important roles on membrane's pore structure and consequently results in different gas transport properties.

Though great progress has been made in the field of carbon membranes, it is not uncommon that a strong trade-off relationship exists between the permeability and selectivity, i.e. the permeation flux through the carbon membranes is considerably reduced as the gas selectivity increases because of the disordered pore structure and diffusion resistance membranes. To tackle this challenging issue, almost all the efforts to control micropores in carbon membrane have been directed toward the production of miroporous molecular sieving carbon (MSC), or synthesis of composite membranes by incorporating some nano-scaled materials such as Ag-nanocluster [9], palladium nano-particles [25], zeolite [26-28], metal oxides [29], carbon nanotubes [30-31] and silica [10,32-33], but it is still far from satisfactory.

To solve this challenging task, here we proposed a simple strategy to incorporate zeolite into the membranes that could significantly improve the gas flux without losing the selectivity of membranes. As a mesoporous zeolite, SBA-15 has a lot of particular characteristics, such as large surface area, narrow pore distribution, long

pore diameter, large pore volume, and high mechanical intensity sustained by a thick wall [34-35], so it is a very ideal tailor for pore structure.

In this study, we reported a method for the preparation of SBA-15 zeolite/carbon nanocomposite membrane. By modifying the carbon matrix with zeolite, we will show that it is possible to increase the selectivity factor notably as the permeability increased abundantly for the gas separation compared to their carbon membrane that were not modified. All these membranes are characterized by FE-SEM and TGA analysis to evaluate the surface morphology and thermal stability of prepared nanocomposite molecular sieve membranes.

2. Experimental

2.1. Preparation of CMS membranes

Preparation of the zeolite-incorporated composite CMS membrane involved three steps. The first step is to prepare the zeolite, siliceous SBA-15, which has been described in detail elsewhere [36]. Pluronic P123 (an amphiphilic triblock copolymer that contains ethylene oxide (EO) and propylene oxide (PO) in the empirical ratio of $EO_{20}PO_{70}EO_{20}$) using as the structure-directing agent was mixed with 2 M HCl under

vigorous stirring at 313 K for 3 h until a clear solution was formed. TEOS (tetraethylorthosilicate, 98%, Merck) was added to the solution under stirring. After 0.5 h, the gel was formed and the stirring was continued at 373 K for 24 h, cooled down to room temperature and filtered under vacuum. It was washed by deionised water three times and was calcined at 773 K for 6 h in air (at a heating rate of 2 K/min). Fig. 1 represents the porous structure and surface image of zeolite. The results of TEM and SEM measurements confirm that the highly ordered mesostructure of SBA-15 can be obtained.

The second step is to prepare the incorporated matrix coating suspension. The coating suspension was prepared by dispersing some zeolite with a media particle size of 1-2 μm into 15 % n-methyl-2-pyrolidone (NMP) solution of PEI. Generally, about 0.2-0.4 g of zeolite particles were used in the 100 ml solution. To disperse the zeolite homogeneously in the solution, a high-intensity ultrasonic processor was used to sonicate the coating suspension for about 30 min. This sonication step provided powerful shearing of the zeolite particles breaking up aggregates of particles and enhancing homogeneity during the intense agitation. After sonication, the coating suspension was allowed to stand for about 6 h to let larger zeolite particles settle to the bottom of a vial.

The third step was to prepare SBA-15/carbon molecular sieve composite membrane (denoted as SBA-15/CMS composite membrane) through spin coating, curing and carbonization. The curing and carbonization trajectory used here was followed the TGA results (see next paragraph). In these processes, the incorporated matrix coating suspension was spread on the macro-porous α-alumina support disk (average pore size: 0.14 μm, diameter: 2.3 mm, porosity: 40-48%) by spin coating technique, resulting in a thin film of the polymer on the support. After coating, the membranes were kept in an isopropyl alcohol–water (1:1 ratio) coagulating bath for 2 h. Then the membranes (denoted as SBA-15/PEI polymeric membrane) were dried in air overnight. Then the polymeric membrane was cured in a tubular furnace under air gas stream from room temperature up to 150 ^{o}C with a heating rate of 0.5 ^{o}C/min and held at this temperature for 1 h. After curing, the membrane was carbonized in inert gas stream from 150 ^{o}C to 500 ^{o}C with a heating rate of 5 ^{o}C/min and kept at this temperature for 1 h. The membranes were carefully taken out from the quartz tube in the furnace and eventually stored in a desiccator containing silica gel.

2.2. Characteristics of polymeric and carbonized membranes

126 The microstructure images of zeolite XAB-15 were recorded with transmission
127 electron microscopy (TEM) analysis. The images were recorded using a JEOL
128 JSF-2000FX transmission electron microscopy (JEOL, Inc., Kyoto, Japan) at an
129 excitation voltage of 200 kV.

130 The thermal stability, i.e. carbon yield, defined as the weight relative to the initial
131 precursor weight, was evaluated by TGA. The TGA experiments were carried out
132 using a Seiko SSC 5000 with a nitrogen atmosphere and flow rates of 50 ml/min. The
133 heating was 10 ^{o}C/min, and the sample was heated to 700 ^{o}C.

134 The distribution of zeolite in the SBA-15/CMS composite membrane was
135 investigated with field-emission scanning electron microscopy (FESEM). The SEM
136 was used to look at both the cross-section and surface of the membranes. The
137 micrographs were obtained using a JEOL JSM-6700F, OXFORD INCA ENERGY
138 400 for magnifications up to 50,000 ratios.

139

140 *2.3. Permeation test*

141

142 To analyze the permeation characteristics of the membrane, different gases were
143 selected: CO_2 (3.3 Å), O_2 (3.46 Å), and N_2 (3.64 Å). The values in brackets
144 correspond to the kinetic diameter of each gas. The gas permeation properties of the

PEI-based CMS membrane and SBA-15/CMS membrane were investigated using a standard vacuum time-lag method at room temperature and a feed pressure of 152 cmHg [32-33]. Before permeation test, the membrane samples were masked using impermeable aluminum tape with a predetermined area (4 cm^2), and then epoxy sealant was carefully applied at the interface between the tape and the CMS membranes to prevent any gas leak. As shown in Fig. 2, the CMS membrane was attached to a permeation cell (25-mm disc filters, Millipore, Billerica, MA, USA), and degasses by exposing both sides of the membrane to vacuum. After degassing, high-purity penetrant supplied from compressed gas cylinders were introduced into the upstream side of the membrane. The variation of pressure in the downstream was recorded by using a pressure transducer (MKS Instrumens, Andover, MA, USA) and digital equipment connected to a computer. The steady-state rate of pressure rise on the downstream side was used to determine the gas permeance properties. The permeability coefficients were expressed in Barrer (1 Barrer = 1×10^{-10} cm^3 (STP) cm cm^{-2} s^{-1} $cmHg^{-1}$). Hence the permeation rate (P) can be calculated by:

$$P = \left(\frac{dp}{dt}\right) \frac{V.T_o}{A.\Delta P} \times \frac{L}{T.P_o} \quad (1)$$

where V is the volume of gas permeation in unit time (cm^3), dp/dt the rate of pressure rise in the steady state, ΔP the pressure difference in the membrane side, A the area of the membrane (cm^2) and L the membrane thickness (cm), P_o being 76 cmHg and T_o

being 273 K, and T the measured temperature (K). In the case of pure penetrant gas, the ideal separation factor of pure gas A/B ($\alpha_{A/B}$) is defined as the ratio of permeation rate of A to that of B, which can be expressed by:

$$\alpha_{A/B} = P_A/P_B \quad (2)$$

The apparent diffusion coefficient, D, is determined from the time-lag, θ, as expressed by:

$$D = L^2/6\theta \quad (3)$$

The apparent solubility coefficient, S, is evaluated as S = P/D.

3. Results and discussion

3.1. Thermal stability of the CMS membrane

The typical TGA profiles for the original PEI precursor, pure PEI polymeric membrane and composite SBA-15/PEI polymeric membrane were shown in Fig. 3. The pure PEI precursor shows three obvious thermal degradation stages. The first thermal degradation stages starts from the temperature of 25-450 ^{o}C with the weight loss ca. 4.5 wt% that is attributed to the minor thermal degradation of branch groups in PEI molecular chains. The second weight loss stage is between 450-540 ^{o}C, which

corresponds to the degradation of functional groups in the main molecular chains. When the thermal degradation temperature is up to 700 ^{o}C the weight loss rate increased and the weight loss is about 70 wt% of the total weight loss due to the completely pyrolysis of carbon structure. Compared to original PEI precursor, pure PEI polymeric membrane shows an additional weight loss stage in the temperature range of 25-200 ^{o}C due to the removal of residual solvent NMP. Fig. 3 also exhibits the thermal degradation profile of composite PEI membrane after incorporating with SBA-15. Although SBA-15/PEI polymeric membrane has a similar thermal weight loss profile as compared to pure PEI polymeric membrane, however, the former presents higher thermal weight loss during the first stage. The huge weight loss of composite polymeric membrane after incorporating SBA-15 was about 20 wt%. Note that this weight loss was significantly higher than the concentration of 2 wt% of the total precursor mass. Furthermore, dispersing SBA-15 into the polymeric membrane by extra ultrasonically dispersing method resulted in more weight loss than only vigorously stirring, which accelerates decomposition of the PEI structure. The results indicated some catalytic degradation effect of zeolite SBA-15 on polymeric membrane structure. The catalytic degradation of SBA-15 in the early stage of pyrolysis procedure would lead to the creation of large amount of micropores in the

matrix (see next paragraph). As the result, the gas permeability of SBA-15 composite CMS membrane would be improved.

3.2. Microstructures of the CMS membrane

Fig. 4 shows the photographs of pure PEI-based CMS membrane and SBA-15/CMS composite membrane. From the FESEM images (Fig. 4 (a)), continuous CMS membrane were formed on the macroporous support by one time spin coating method. The thickness of the CMS membrane was about 2 μm, and the surface of CMS membrane exhibits a very smooth being almost dense structure (Fig. 4 (b)). Compared to the pure CMS membrane, interestingly, the SBA-15/CMS membrane shows large amount of micropores in the surface structure (Fig. 4(c)) after pyrolysis at the same condition. The result suggests that the dispersion of zeolite SBA-15 particle in the polymer precursor may result in catalytic degradation effect of the SBA-A5 particles on pyrolysis stages and acceleration the rate of decomposition the PEI structure. Also seen from the FESEM image of SBA-15/CMS composite membrane (Fig. 4(d)), the white spots are SBA-15 zeolite particle that are dispersed in the carbon matrix. The enchased SBA-15 zeolite would provide two functions to improve the gas permeability of the composite carbon membrane: one is providing

large amount of gas diffusion channels in their interior ordered porous structure; the other is developing phase gap between the interfaces of SBA-15 and carbon matrix. By those diffusion channels and interfacial gaps, gases can be more easily permeated through carbon membrane and high capacity membranes may create [37]. Therefore, from the SEM images suggest that the incorporation of SBA-15 into the PEI does markedly change the microstructure of resulting carbon membranes.

3.3. Gas permeation performance

The gas permeation results for carbon dioxide, oxygen and nitrogen, and the ideal separation factors of other gases to nitrogen are summarized in Table 1. The pure gas permeabilities through the SBA-15/CMS composite membrane were almost higher for all gases than those of pure CMS membranes. In this study, we put emphasis on the change in the gas permeation properties through the SBA-15/CMS membranes caused by textural changes in the final carbonized membrane. Although the pure CMS and SBA-15/CMS membrane used the same polymer as the precursor, the different pore textural of the porous SBA-15 zeolite greatly influenced the gas transport behavior of the membranes. From the gas permeation results shown in Table 1, the improvement in gas permeabilities for SBA-15/CMS membrane seems

attributed to the reduction of gas transport resistance through membranes by providing additionally microporous channels in SBA-15 and interfacial resistance [37-38]. Furthermore, the gas selectivity of these membranes was not losing after incorporating SBA-15 into the membrane. As can be seen from previous FESEM images and XRD patterns, the final carbon structure form more porous or less compact structures in the carbon matrix might be responsible for higher gas permeability without losing selectivity in the SBA-15/CMS membrane.

The gas permeability of SBA-15/CMS composite membrane also follows an order of $CO_2 > O_2 > N_2$, which is correlated with their kinetic diameter (CO_2 (0.33 nm), O_2 (0.346 nm), and N_2 (0.364 nm)) instead of the molecular weight of gas molecules. The higher selectivity than those expected from Knudsen diffusion are achieved confirms that the gas permeation through the composite carbon membranes obeys molecular sieving mechanism and some pores of the prepared carbon membrane are of molecular dimensions. The SBA-15 zeolite size is likely to affect both the pore size distribution and the micropore volume (selectivity and permeability).

Further information regarding the gas transport properties of the SBA-15/CMS membrane was obtained by carrying out permeation experiments with different feed pressure. The pressure dependence on gas permeability through PEI-based CMS

membranes and SBA-15/CMS membranes are also showing in Table 1. As shown, it can be seen that various gas permeabilities hardly changed with different pressure. A similar behaviour was reported by Wu and Yuan [40]. The result can be of considerable importance for determining the optimum operating condition and indicates that this membrane can be operate under high feed pressure for increasing gas flux without formatting any defect or crack.

The gas diffusion coefficient and the solubility coefficient through pure CMS membranes and SBA-15/CMS membranes are summarized in Table 2. The CO_2, O_2 and N_2 diffusion coefficients through the SBA-15/CMS membrane were lower than those through pure CMS membrane, while the solubility coefficients through the SBA-15/CMS membrane were higher than those through pure CMS membrane. The larger solubility coefficients are mainly attributed to the increase in the overall gas permeability. This implies that the gas transport through these membranes was favorably achieved through the SBA-15 zeolite, and also that the surface properties of the SBA-15 zeolite influenced the interacting between gas molecular and zeolite. However, as shown in Table 3, note that this faster solubility of gases through SBA-15/CMS membrane decreases the solubility selectivity in comparison with that of pure CMS membrane. Moreover, SBA-15/CMS membrane was shown to exhibit diffusivity selectivity 21.7 times greater than CMS membrane for O_2/N_2 separation.

The higher diffusion selectivity of molecular sieving media is based primarily on the ability to limit rotational degrees of freedom of bigger gas molecular in the diffusion transition state while allowing free rotation for the smaller one [39]. SBA-15 zeolite accomplishes this by the presence of constricted windows to perform precise size selection of penetrants.

4. Conclusions

In the present work, we have shown that SBA-15 zeolite is a good tailor for modification the pore structure of carbon membrane, which results a high-performance membrane for improved gas separation. The selective SBA-15/carbon domain presents a structure with pores of molecular dimension and provides an interface improved the interacting between gas molecular and passageway. Finally, we can say that using SBA-15 zeolite as modifier having a uniform porous structure and silica composition provides an additional clue to improve CO_2 gas permeability by sorption mechanism, while O_2 gas permeability by diffusion mechanism.

Reference

[1] K.K. Sirkar, H. Winston, Part I and Part II Membrane Hand book (1992) 1.

[2] T.A. Centeno and A.B. Fuertes, J. Membr. Sci. 160 (1999) 201.

[3] F.K. Katsaros, T.A. Steriotis, A.K. Stubos, A. Mitropoulos, N.K. Kanellopoulos and S.R. Tennison, Microporous Mater. 8 (1997) 171.

[4] W. Yuan, Y.S. Lin and W. Yang, J. Am. Chem. Soc. 126 (2004) 4776.

[5] K.M. Steel and W.J. Koros, Carbon. 43 (2005) 1843.

[6] Y.M. Park and Y.M. Lee, Adv. Mater. 17 (2005) 477.

[7] S.M. Saufi and A.F. Ismail, Carbon 42 (2004) 241.

[8] G. Arora and S.I. Sandler, Fluid Phase Euqilibria 259 (2007) 3.

[9] J.N. Barsema, J. Balster, V. Jordan, N.F.A. van der Vegt and M. Wessling, J. Membr. Sci. 219 (2003), 47.

[10] A.F. Ismail and L.I.B. David, J. Membr. Sci. 193 (2001) 1.

[11] N. Kishore, S. Sachan, K.N. Rai and A. Kumar, Carbon 41 (2003) 2961.

[12] J.N. Barsema, N.F.A. Van der Vegt, G.H. Koops and M. Wessling, J. Membr. Sci. 205 (2002) 239.

[13] H. Hatori, T. Kobayashi, Y. Hanzawa, Y. Yamada, Y. Iimura, T. Kimura and M. Shiraishi, J. Appl. Polym. Sci. 79 (2001) 836.

[14] A.B. Fuertes, D.M. Nevskaia and T.A. Centeno, Micropor. Mesopor. Mater. 33 (1999) 115.

[15] S. Niyogi and B. Adhikari, Euro. Poly. J. 38 (2002) 1237.

[16] Y. Xiao, T.S. Chung, H.M. Guan and M.D. Guiver, J. Membr. Sci. 302 (2007) 254.

[17] L.I.B. David and A.F. Ismail, J. Membr. Sci. 213 (2003) 285.

[18] H. Kita, H. Maeda, K. Tanaka and K. Okamoto, Chem. Lett. 2 (1997) 179.

[19] F.K. Katsarov, T.A. Steriotis, A.K. Stubos, A. Mitropoulos, N.K. Kanellopoulos and S. Tennison, Micropor. Mater. 8 (1997) 171.

[20] M.B. Shiflett and H.C. Foley, Science 285 (1999) 1902

[21] H. Wang, L. Zhang and G. Gavalas, J. Membr. Sci. 177 (2000) 25.

[22] C. Song, T. Wang, X. Wang, J. Qiu and Y. Cao, Sep. Purf. Technol. (2007) (In press) (doi: 10.1016/j.seppur.2007.05.019)

[23] M.G. Sedigh, L. Xu, T.T. Tsotsis and M. Sahimi, Ind. Eng. Chem. Res. 38 (1999) 3367.

[24] T.A. Centeno and A.B. Fuertes, Carbon 38 (2000) 1067.

[25] H. Suda, S. Yoda, A. Hasegawa, T. Tsuji, K. Otake and K. Haraya, Deaslination 193 (2006) 211.

[26] Z.H. Zhou, J.H. Yang, L.F. Chang, Y. Zhang, W.G. Sun and J.Q. Wang, Chinese Chem. Letters 18 (2007) 455.

[27] Z. Zhou, J. Yang, Y. Zhang, L. Chang, W. Sun and J. Wang, Sep. Purif. Technol. 55 (2007) 392.

[28] X. Zhang, W. Zhu, H. Liu and T. Wang, Materials Letters 58 (2004) 2223.

[29] M. Yoshimune, I. Fujiwara, H. Suda and K. Haraya, Desalination 193 (2006) 66.

[30] P.S. Rao, M.Y. Wey, H.H. Tseng, I. Arun Kumar and T.H. Weng, Micropor. Mesopor. Mater. (2008), doi:10.1016/j.micromeso.2007.12.008.

[31] H.H. Tseng, I. Arun Kumar, T.H. Weng, C.Y. Lu and M.Y. Wey, Desalination 000 (2009) 1-6.

[32] H.B. Park, C.H. Jung, Y.K. Kim, S.Y. Nam, S.Y. Lee and Y.M. Lee, J. Membr. Sci. 235 (2004) 87.

[33] H.B. Park, S.Y. Lee and Y. M. Lee, J. Molecular Structure 739 (2005) 179.

[34] X. Liao, Z. Zhou, Z. Wang, X. Zou, G. Liu, M. Jia and W. Zhang, J. Colloid Interface Sci. 308 (2007) 176.

[35] Z. Gao, L. Wang, T. Qi, J. Chua and Y. Zhang, Colloids and Surfaces A: Physicochem. Eng. Aspects 304 (2007) 77.

[36] A.A. Campos, L. Martins, L.L. de Oliveira, C.R. da Silva, M. Wallau, E.A. Urquieta-Gonza´lez, Catal. Today 107–108 (2005) 759.

[37] B. Zhang, T. Wang, Y. Wu, Q. Liu, S. Liu, S. Zhang and J. Qiu, Sep. Puri. Technol. 60 (2008) 259.

[38] Y. Li, T.S. Chung, C. Cao and S. Kulprathipanja, J. Membr. Sci. 260 (2005) 45.

[39] C.M. Zimmerman, A. Singh and W.J. Koros, J. Membr. Sci. 137 (1997) 145-154.

[40] J. Wu and Q. Yuan, J. Membr. Sci. 204 (2002) 185-194.

356

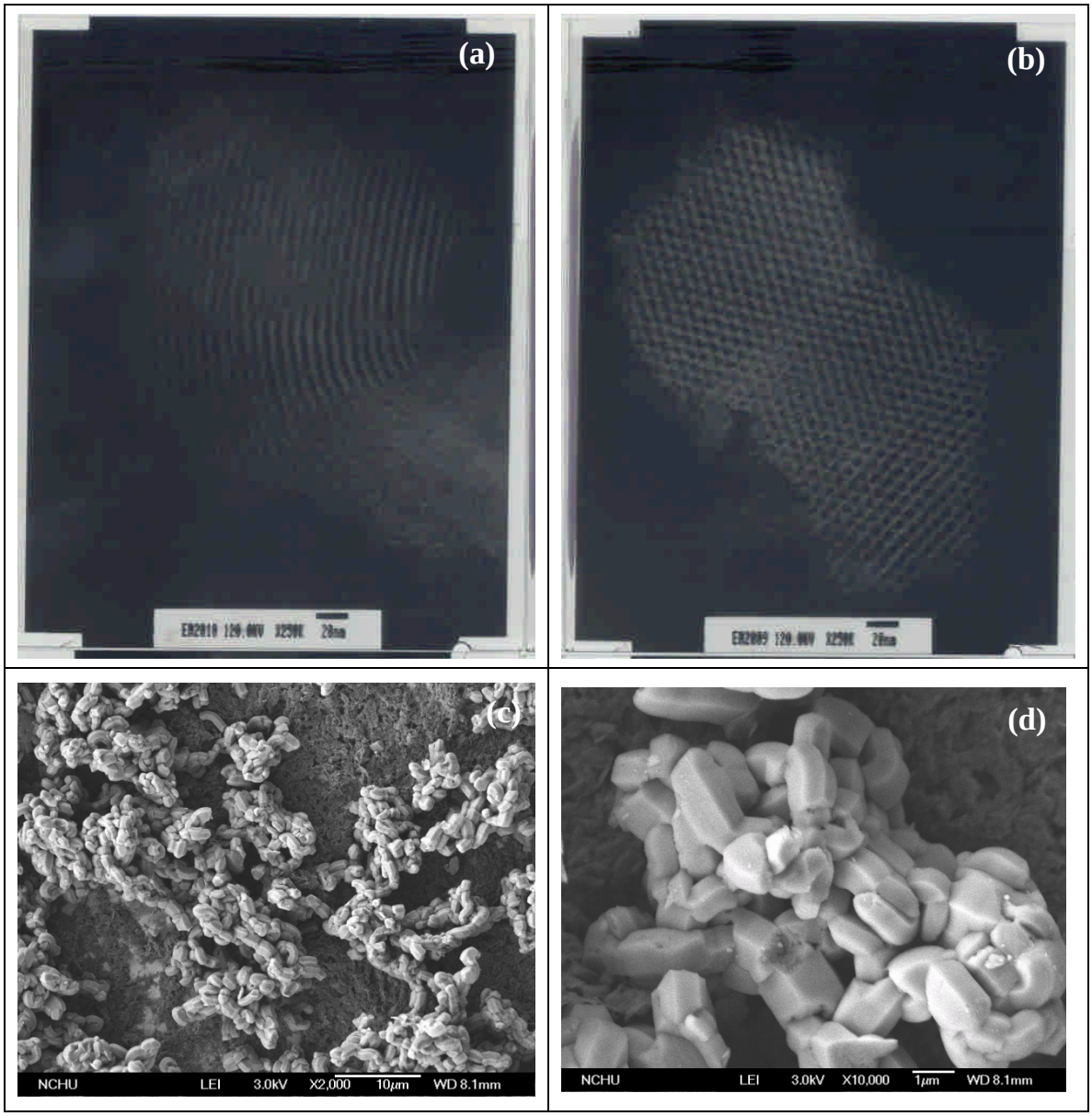

357 Fig. 1. TEM (a and b) and FESEM (c and d) images of SBA-15 zeolite.

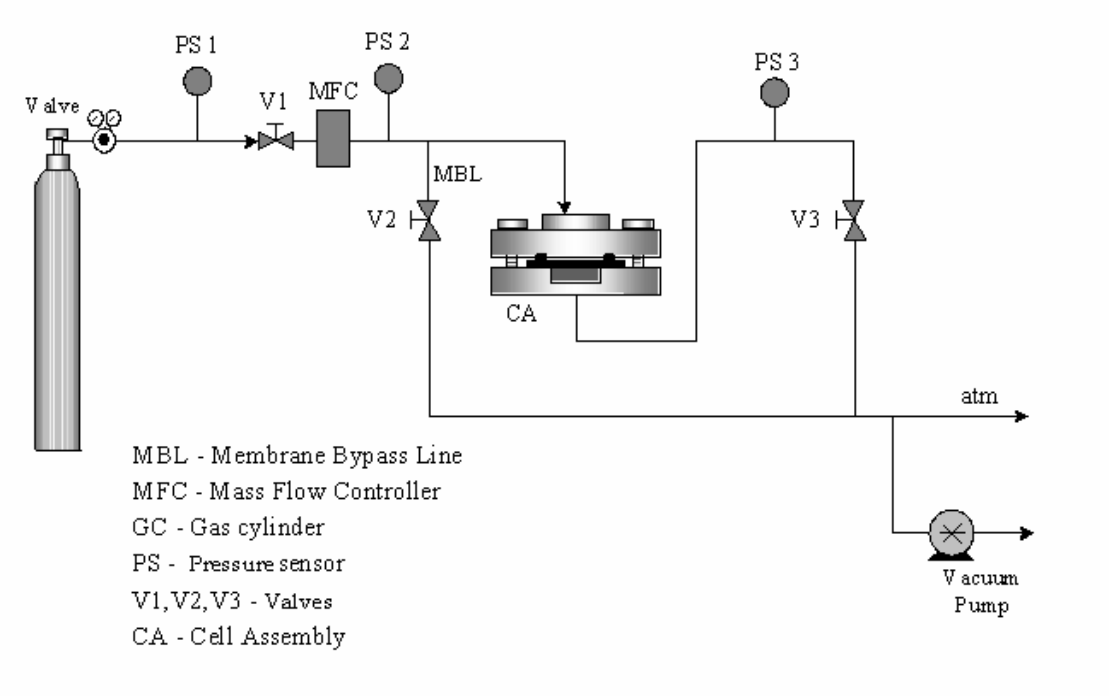

358

359 Fig. 2. Diagram of system to analyze the permeation of pure gases.

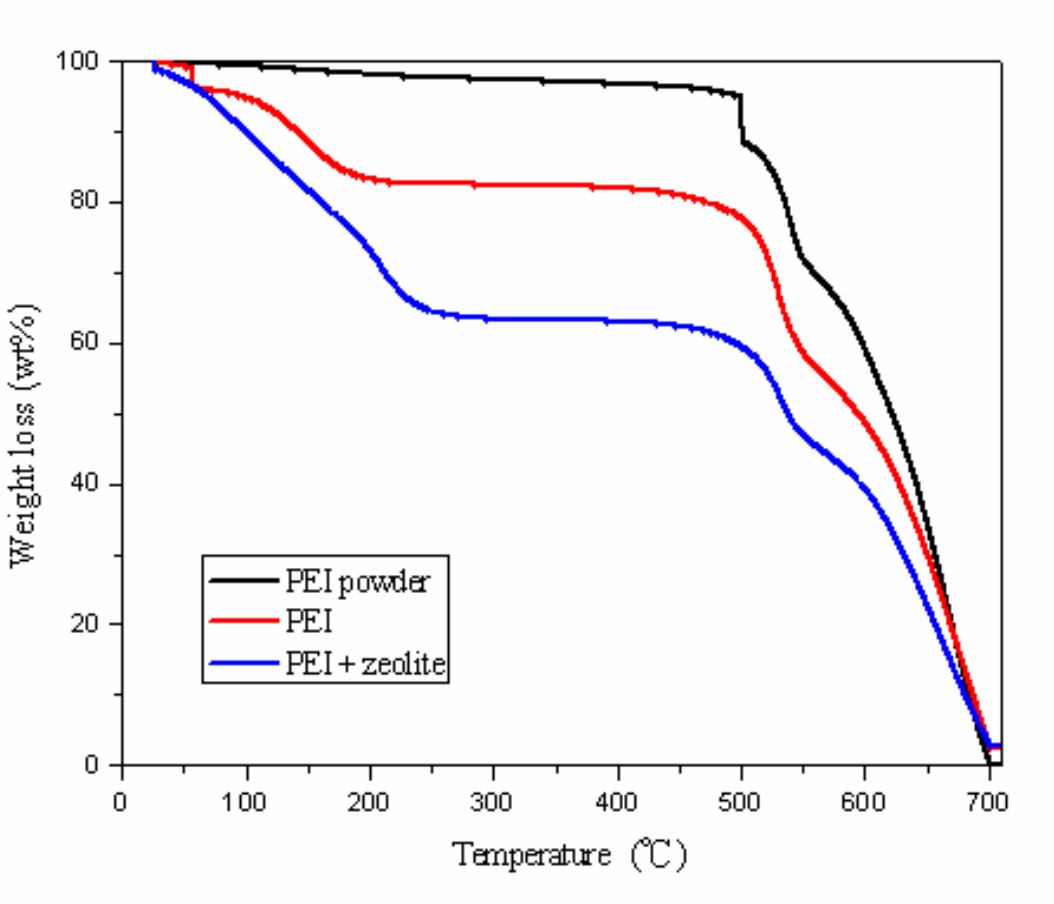

360

361 Fig. 3. Thermal weight loss of pure PEI and SBA-15/PEI polymeric membranes.

362

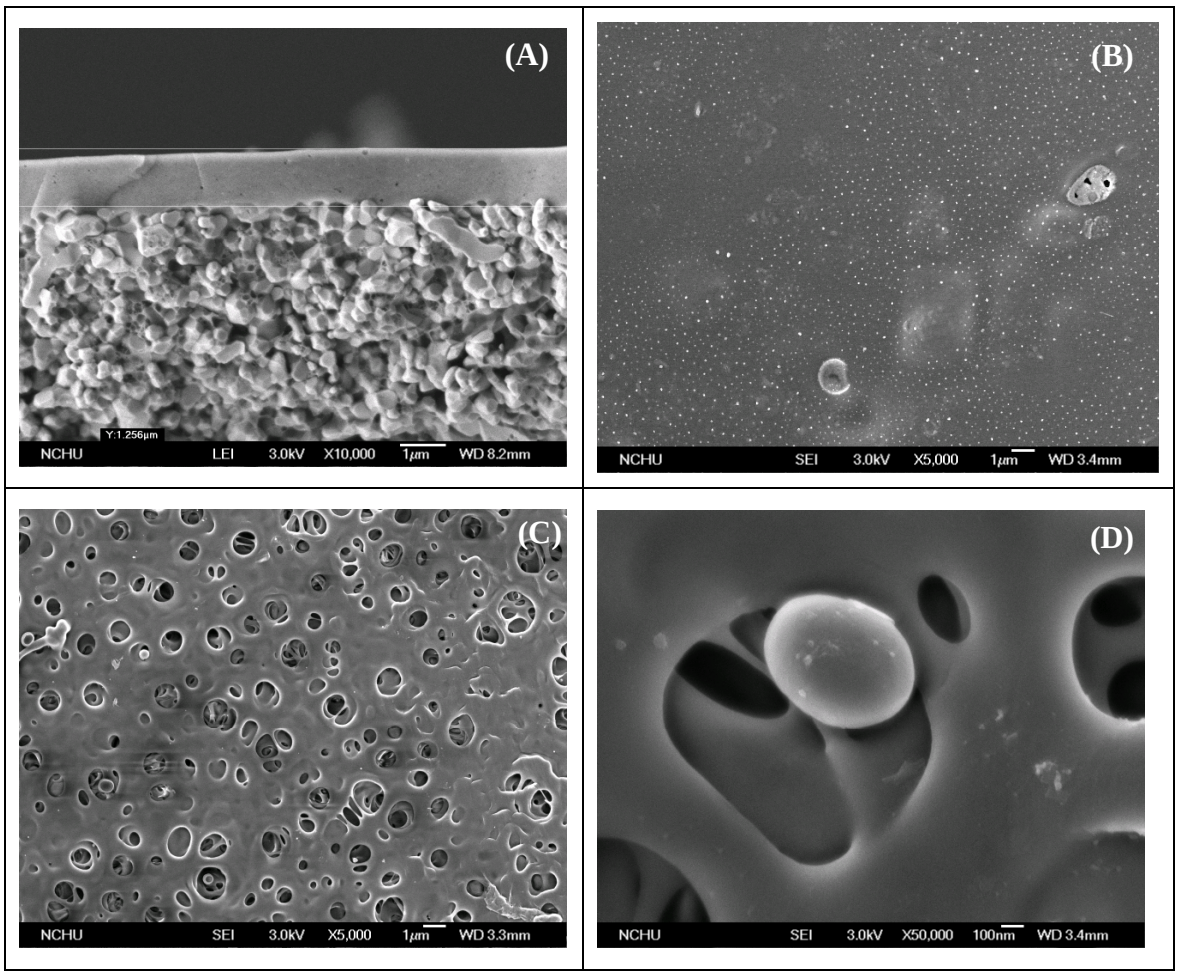

363 Fig. 4. FESEM images of PEI-based CMS membrane (A and B) and SBA-15/CMS

364 membrane (C and D).

365 Table 1

366 Gas permeabilites and selectivities measured at 299 K for the PEI-based CMS and

367 SBA-15/CMS membrane

	Feed pressure	Permeability (Barrer)			Ideal separation factor	
		CO_2	O_2	N_2	CO_2/N_2	O_2/N_2
CMS	1	963	484	121	7.9	4.0
	3	743	365	159	4.7	2.3
SBA-15/CMS	1	1271	306	262	4.8	1.2
	3	1144	422	189	6.1	2.3

368

Table 2

Diffusion coefficient and solubility coefficient of pure CMS and SBA-15/CMS membranes at different feed pressure and 26 ^{o}C

	Feed pressure	Diffusion coefficient (10^{-8} cm^2/s)			Solubility coefficient (1/cmHg)		
		CO_2	O_2	N_2	CO_2	O_2	N_2
Pure CMS	1	13.6	13.1	15.8	71.0	37.0	7.6
	3	43.8	12.1	17.0	17.0	30.2	9.3
SBA-15/CMS	1	1.8	4.0	0.7	712.2	70.4	394.2
	3	1.8	10.1	0.7	632.0	41.4	282.5

373 Table 3

374 Diffusion selectivity and solubility selectivity of pure CMS and SBA-15/CMS

375 membranes at different feed pressure and 26 ^{o}C

	Feed pressure	Diffusion selectivity (10^{-8} cm^2/s)		Solubility selectivity (1/cmHg)	
		$D(CO_2)/D(N_2)$	$D(O_2)/D(N_2)$	$S(CO_2)/S(N2)$	$S(O2)/S(N_2)$
Pure CMS	1	0.86	0.83	9.28	4.84
	3	2.57	0.71	1.82	3.25
SBA-15/CMS	1	2.69	6.02	1.80	0.19
	3	2.71	15.26	2.23	0.15

376

研究成果自評

本研究內容與原計畫相符，所有預期目標皆已達成；研究成果因添加沸石（SBA-15）對碳分子篩選薄膜作改質，而有效地提升氣體的滲透率與選擇率；此外薄膜的熱穩定性及抗壓強度亦因沸石的添加而提升。因此不論就學術成果或應用價值，皆適合在學術期刊發表或申請專利。目前已將研究成果撰寫成期刊論文格式準備投稿，專利申請亦在準備中。

出席國際學術會議心得報告

計畫編號	NSC 96-2221-E-040-001
計畫名稱	修正碳分子篩選薄膜之微孔結構及其於氣體分離特性之應用
出國人員姓名 服務機關及職稱	曾惠馨 中山醫學大學/職業安全衛生學系暨碩士班
會議時間地點	August 18-22, 2008, Tokyo-JAPAN
會議名稱	10th International Conference on Inorganic Membranes
發表論文題目	Novel zeolite/polyimide derived carbon molecular sieve membrane with high permeance for gas separation

一、參加會議經過

研究人員此次前往日本東京，參加由日本薄膜協會及早稻田大學（Waseda university）於 2008 年八月 18 日至 22 日所舉辦的「ICIM10：第十屆國際無機薄膜研討會」(10th International Conference on Inorganic Membranes)。

該無機薄膜研討會每二年舉辦一次，並邀請知名專家學者進行演講與分享其在無機薄膜領域之研究經驗與心得，與會者包含工業界與學術界，共計約數百名。

二、與會心得

討論的議題共分為：無機薄膜（silica and other oxide ceramics、zeolites、metals、carbon and other non-oxide ceramics、proton and oxygen ion conducting ceramics、inorganic-organic hybrids）、無機薄膜的應用（industrial applications、gas separation、pervaporation、microfiltration/ultrafiltration/nanofiltration、fuels cells、catalysis in inorganic membranes、biochemical and biomedical application、sensor application and membrane miniaturization、novel applications）、性質與模擬（Properties and modeling、Transport properties and separation mechanisms、Chemical structural and thermodynamic properties、Reactor modeling that includes membrane characteristics、Membrane characterization、Scaling up）等兩大主題，與會者均可全程參與，瞭解各方面的趨勢與發展。以下依據與研究人員較相關之研究領域的各主題討論內容之心得作一綜合性摘要。

1. 燃料電池與離子選擇性薄膜方面：近年來質子交換膜燃料電池，因，而被視為最具發展潛力之燃料電池，然目前仍面臨下列問題：(1)因氫氣儲存技術：一般使用高壓鋼瓶或儲氫合金，但有成本、重量、安全性等不利因素；(2)成本高 ：其觸媒層所使用的貴金屬-鉑其費用和供貨不確定性增加成本；(3)氫的來源：重組後的燃料內含有一氧化碳和其他污染物；(4)氧還原反應的效率低：受到觸媒載體性質、合成方法等許多因素的影響。而在此次會議發表的論文中，有多篤皆與該主題有關，並提出下列方法，以解決目前質子交換膜燃料電池所面臨的問題：(1)使用雙金屬觸媒如：Pt-Ru、Pt-Sn；(2)金屬觸媒中加入氧化物，如:ZrO_2、CeO_2；(3)先行將重組器所產生的燃料，

經過附有觸媒及少量 O_2 或空氣的反應槽；(4)添加少量的氧化劑一起進入陽極，產生氫氧根，把附著在鉑表面的 CO 氧化成 CO_2 等。因此在薄膜中添加金屬觸媒以提升對 H_2 的選擇率則為較新穎之研發技術。

2. 氣體與揮發性有機化合物的分離方面：就與會中所發表之論文而言，現今較常應用於氣體與揮發性有機化合物分離的薄膜材料包含有高分子薄膜、及以沸石、金屬為基礎的無機薄膜，而與本人研究相關的碳分子篩選膜則僅見一篇。其應用領域除富氮或富氧之氣體分離外，引發的溫室效應之氣體的分離，或提升替代性能源氣體之純度，亦為日後應用之重點方向。
3. 滲透蒸發方面：近年來由於替代能源之漸受重受，及半導體場所產生的大量有機廢溶劑等問題，因此利用滲透蒸發技術，將有機溶劑與水分離之技術已漸受重視，其因下列特色，而具有取代傳統化工程序中蒸餾分離之潛力，

三. 攜回資料：論文摘要一本、論文全文光碟一片、識別證。